

Jet - Underlying Event Separation Method for Heavy Ion Collisions at the Relativistic Heavy Ion Collider

J. A. Hanks¹, A. M. Sickles², B. A. Cole³, A. Franz², M. P. McCumber⁴, D. P. Morrison²,
 J. L. Nagle⁴, C. H. Pinkenburg², B. Sahlmueller¹, P. Steinberg², M. von Steinkirch¹, M. Stone⁴
¹ *Department of Physics and Astronomy, Stony Brook University, SUNY, Stony Brook, New York 11794-3400, USA*
² *Physics Department, Brookhaven National Laboratory, Upton, New York, 11973-5000*
³ *Columbia University, New York, New York 10027 and Nevis Laboratories, Irvington, New York 10533, USA and*
⁴ *University of Colorado, Boulder, Colorado 80309, USA*
 (Dated: June 3, 2019)

Reconstructed jets in heavy ion collisions are a crucial tool for understanding the quark-gluon plasma. The separation of jets from the underlying event is necessary particularly in central heavy ion reactions in order to quantify medium modifications of the parton shower and the response of the surrounding medium itself. There have been many methods proposed and implemented for studying the underlying event substructure in proton-proton and heavy ion collisions. In this paper, we detail a method for understanding underlying event contributions in Au+Au collisions at $\sqrt{s_{NN}} = 200$ GeV utilizing the HIJING event generator [1]. This method, extended from previous work by the ATLAS collaboration [2], provides a well-defined association of “truth jets” from the fragmentation of hard partons with “reconstructed jets” using the anti- k_T algorithm. Results presented here are based on an analysis of 750M minimum bias HIJING events. We find that there is a substantial range of jet energies and radius parameters where jets are well separated from the background fluctuations (often termed “fake jets”) that make jet measurements at RHIC a compelling physics program.

I. INTRODUCTION

Understanding the detailed interaction and coupling between hard scattered partons and the quark-gluon plasma through which they propagate is essential to our fundamental knowledge of QCD and in determining properties of the quark-gluon plasma. The measurement of fully reconstructed jets in heavy ion collisions at the LHC [3, 4] highlight the substantial additional information contained therein and its complementary nature to single hadron [5–7], di-hadron correlations [8–11]. The measurement of direct photon-jet correlations is another critical handle to be utilized [12]. Extending fully calorimetric jet measurements to lower center-of-mass energies at the Relativistic Heavy Ion Collider provides measurements for kinematics difficult to access at the LHC and the QGP at different temperature and coupling regime.

With the first Pb+Pb at $\sqrt{s_{NN}}=2.76$ TeV collisions at the LHC new insights into jet physics in heavy ion collisions were gained. The ATLAS collaboration reported an increase in the number of energy asymmetric di-jets in central Pb+Pb collisions compared to proton-proton and peripheral Pb+Pb collisions [3]. They also reported the suppression of jets with $100 < p_T < 200$ GeV/c by a factor of approximately when comparing central to peripheral Pb+Pb collisions [13]. The CMS collaboration measured jet-hadron correlations in a similar jet p_T range and found that the energy lost by high p_T fragments was approximately balanced by very low p_T tracks far from the jet axis [4]. However the data from both RHIC and the initial LHC results are not enough to constrain the physics of jet quenching. Most theoretical descriptions have relied on weakly coupled tech-

niques [14]. Features of strong coupling, as observed in descriptions of the bulk matter, might contribute to jet quenching as well. More data on jet observables (including dijet, γ -jet and heavy flavor tagged jets) at RHIC and the LHC will be necessary to understand the physics of jet quenching over the full range of medium properties and jet kinematics and probe for sensitivity of the quenching to outgoing parton virtuality.

The multiplicity of charged particles $dN_{ch}/d\eta$ is approximately 2.15 times higher for Pb+Pb central collisions at $\sqrt{s_{NN}} = 2.76$ TeV compared with Au+Au central collisions at $\sqrt{s_{NN}}=200$ GeV [15]. Thus the soft particle background is substantially higher for LHC events. However, the jet cross section is substantially higher as well, and measurements for jets with energies greater than 100 GeV appear well separated from the background (though detailed publications of these studies are not yet available). Various methods have been explored at the LHC and RHIC for understanding the underlying event contributions, and what are often referred to as “fake jets” [2, 16–18].

At $\sqrt{s_{NN}}=200$ GeV the projected jet rates into $|\eta| < 1$ based on NLO pQCD cross sections [19] and expected RHIC luminosities have been computed [20]. In a typical year of RHIC running 50B Au+Au events could be sampled. In the top 20% centrality that would lead to approximately 10^7 jets above 20 GeV, 10^6 jets above 30 GeV, 10^5 jets above 40 GeV and 10^4 jets above 50 GeV. Over 60% of the time there is full containment of the opposing dijet for 20 GeV jets with that percentage increasing with increasing jet energy.

In this paper, we present a study of jet reconstruction and separation from the underlying event using the HIJING [1] event generator for Au+Au events at

$\sqrt{s_{NN}}=200$ GeV. This follows an iterative underlying event subtraction procedure extended from one developed by the ATLAS Collaboration [2]. While the exact definition of a correctly reconstructed jet versus a “fake jet” is arbitrary, this methodology allows us to make a well-defined and documented comparison to cross-check with other methods.

II. JET - UNDERLYING EVENT SEPARATION METHODOLOGY

For these studies we utilize the HIJING (version 1.383) event generator run with standard settings and quenching turned off for Au+Au collisions at $\sqrt{s_{NN}}=200$ GeV. HIJING is a QCD based Monte Carlo for the study of jet production in high energy nucleus-nucleus collisions. For these initial studies, we explore what a “perfect” detector is capable of measuring. We assume a segmentation in $\Delta\eta \times \Delta\phi = 0.1 \times 0.1$ and that all particle energies are recorded perfectly (with the exception of neutrinos and muons). We assume a nominal coverage of $|\eta| < 1.0$ and full azimuthal coverage. For the entire study we utilize the anti- k_T jet reconstruction algorithm [21] (part of the FastJet package [22]) with radius parameters $R=0.2$, 0.3 , and 0.4 .

A schematic diagram of the underlying event subtraction steps is shown in Fig. 1. The first step is to run the anti- k_T algorithm over the full set of energy values (unsubtracted) with $R=0.2$ and record the jet axis coordinates in η and ϕ . This initial suite of jet candidates is used to exclude regions around these jets from the initial underlying event average energy. Exclusion regions are defined by $R=0.2$ jets in which the maximum tower in the jet has an energy of more than three times the average tower energy in the jet. We then exclude all energies for 0.1×0.1 cells whose center coordinate is within $\Delta R = \sqrt{\Delta\eta^2 + \Delta\phi^2} < 0.4$ of any of the above initial jet candidates. The remaining energy values are used to determine the average cell energy (i.e. in the non-jet regions) in $\Delta\eta = 0.1$ strips. The modulation in the background due to flow must first be removed, so the $\langle \cos(2\phi) \rangle$ (i.e. v_2 parameter) is also determined for the energy distribution and removed from each cell before determining the average. Only the η strips which have complete ϕ coverage after the determination of the exclusion regions are used in the v_2 determination.

The HIJING generator has no bulk collective flow and thus has only a modest $\langle \cos(2\phi) \rangle$ from decays, di-jet correlations and global momentum conservation. As the flow modulation of the underlying event is an important component of any subtraction procedure on real data, we have added a flow modulation to the individual HIJING particles prior to segmenting the energies into cells. The flow parameterization [23] is based on fits to the available data. Higher flow moments have an increasing relative importance for more central events [24], and can be incorporated in future studies.

This underlying event average energy is a zeroth order estimate since the initial jet determination does not have an underlying event subtraction. We now subtract the v_2 modulated underlying event energy cell-by-cell from the cells contained by the initial set of $R=0.2$ jets to get a better estimate of the jet E_T . At this second iterative step, new exclusion regions are defined by towers with $\Delta R < 0.4$ around background subtracted jets with $E_T > 20$ GeV. The underlying event and v_2 are re-determined removing towers within $\Delta\eta < 0.4$ of the jets as described above and the background re-subtracted from the original unsubtracted towers. Finally the anti- k_T jet algorithm is run on the background subtracted towers with a range of R values ($0.2, 0.3, 0.4$).

When the jet reconstruction is run over background subtracted towers many of the towers have negative E_T . We modify these towers to have a small positive energy before passing them to the jet reconstruction algorithm. After the towers are grouped into jets we recalculate the jet E_T including the negative energy.

III. HIJING TRUTH INFORMATION

In order to identify “true jets” from the HIJING event generator, we have augmented the code so that every time the fragmentation routine (HIJFRG) is called, we record the set of final state hadrons that result from that fragmentation. We then run the anti- k_T algorithm on those final state hadrons (using their exact momentum vectors). The jet reconstruction is run once for each anti- k_T jet R parameter under consideration and the resulting “true jet” information is added to the output.

Before presenting the results, it is important to define our terms. Even in a model such as HIJING where all truth information is known, there is an arbitrariness in the definitions of “fake jets” and “true jets” as examples. For example, consider a HIJING fragmentation call that results in hadrons reconstructed via anti- k_T with $R = 0.4$ into a jet with an energy of 20 GeV. If after running jet reconstruction over the full HIJING event one reconstructs a jet using anti- k_T with $R = 0.4$ that has a jet axis within $\Delta R \equiv \sqrt{\Delta\eta^2 + \Delta\phi^2} < 0.25$ and energy 18 GeV, common sense might dictate that this was a “true jet” and the 2 GeV difference is a result of the fluctuations in the underlying event. However, imagine that the HIJING fragmentation reconstructed to an energy of 4 GeV and the full HIJING event resulted in a jet along the same axis but with energy of 40 GeV. Common sense might dictate that this was a “fake jet” (i.e. a very small jet that combined with substantial background fluctuations that results in a very large energy reconstruction).

Here, we define a “fake jet” as one where the associated HIJING fragmentation jet is less than 5 GeV (or does not exist at all). The jet is a good “true jet” if there is an associated HIJING fragmentation jet within $\Delta R = \sqrt{\Delta\eta^2 + \Delta\phi^2} < 0.25$ and greater than 5 GeV. We then examine in detail the HIJING fragmentation jet en-

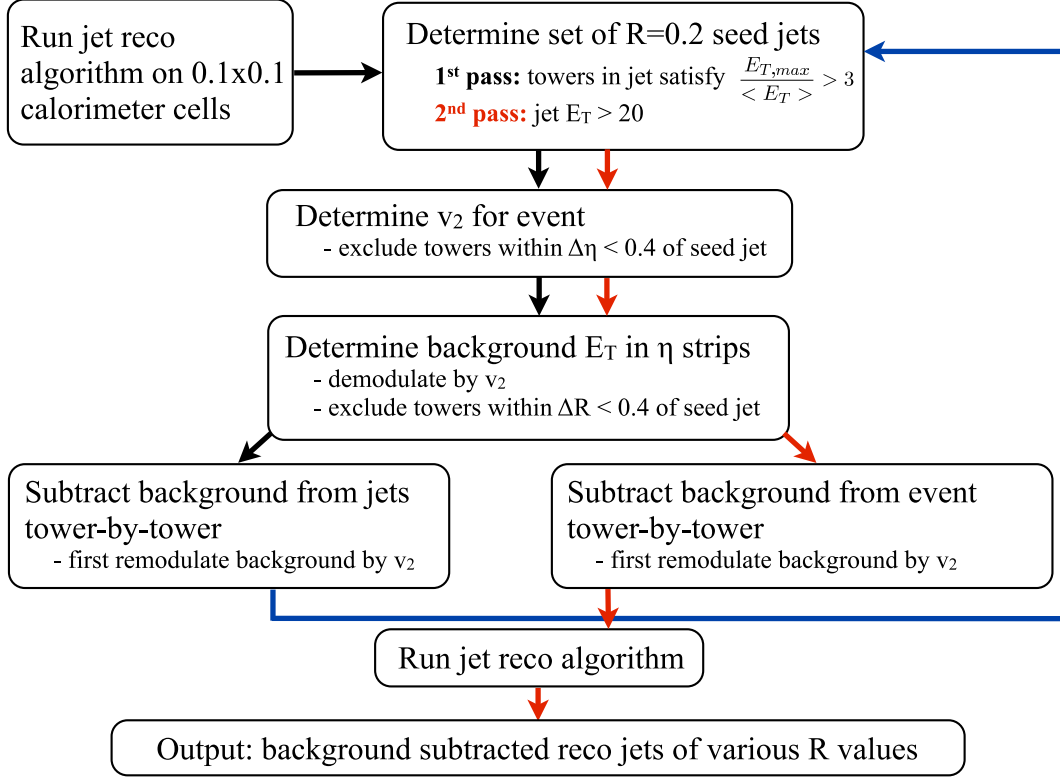


FIG. 1: Schematic illustration of the jet background subtraction method.

ergy distribution for those associated with different selected fully reconstructed jet energies. In principle, one could introduce no such arbitrary definition and put everything into a response matrix down to the lowest energy scales. In practice, if there are substantial contributions of very low energy HIJING fragmentation jet energies to high energy reconstruction jets it will be nearly impossible to control the systematics and unfold such a matrix.

Results presented here are based on an analysis of 750M minimum bias HIJING events.

IV. RESULTS

In order to illustrate the background subtraction procedure, we show a selection of event displays. Figure 2 shows a true dijet pair with $R = 0.2$ where both jets have been matched to reconstructed jets. The reconstructed jet has an axis within $\Delta R < 0.1$ of the true. Also shown in the event are the next highest E_T reconstructed jet. This jet is not matched to any true jets with $E_T > 5$ GeV and has E_T in the region where we expect fake jets to dominate. Figure 3 shows a fake jet with $E_T = 30$ GeV which is not matched to any true jet from the HIJING event. One other fake jet, also not matched to any true jets, is shown on the plot.

We concentrate on central collisions where the underlying event background is largest. For this study we define collision centrality in the HIJING events by the number of charged particles with pseudorapidity $3 < \eta < 4$. Figure 4 shows the efficiency of finding matches to true jets in the most central 10% of collisions for the various anti- k_T R parameters as a function of the true jet E_T . For all R parameters the efficiency rises with jet E_T and approaches 100% between 20 and 30 GeV.

However, in order to quantify the jet performance we need to understand the contribution to the reconstructed jet E_T spectrum from jets which are not matched to any true HIJING jet, “fake jets”. In Figure 5 we show the true, reconstructed and fake jet E_T spectra for $R = 0.2$ (left), 0.3 (middle) and 0.4 (right) for the 10% most central Au+Au at $\sqrt{s_{NN}} = 200$ GeV HIJING events. Shown as red are the true HIJING fragmentation jet distributions. The points show the final reconstructed jet distribution. This is broken down into those jets that are matched with a true HIJING jet and those that are not matched with a true HIJING jet. To be considered matched the jet axis of the reconstructed jet must be within $\Delta R < 0.25$ of the true HIJING jet and the HIJING jet must have $E_T > 5$ GeV. One observes a good match between true HIJING and matched reconstructed jet distributions taking into account the additional energy resolution blurring from the underlying event subtraction. One observes a very large contribution frac-

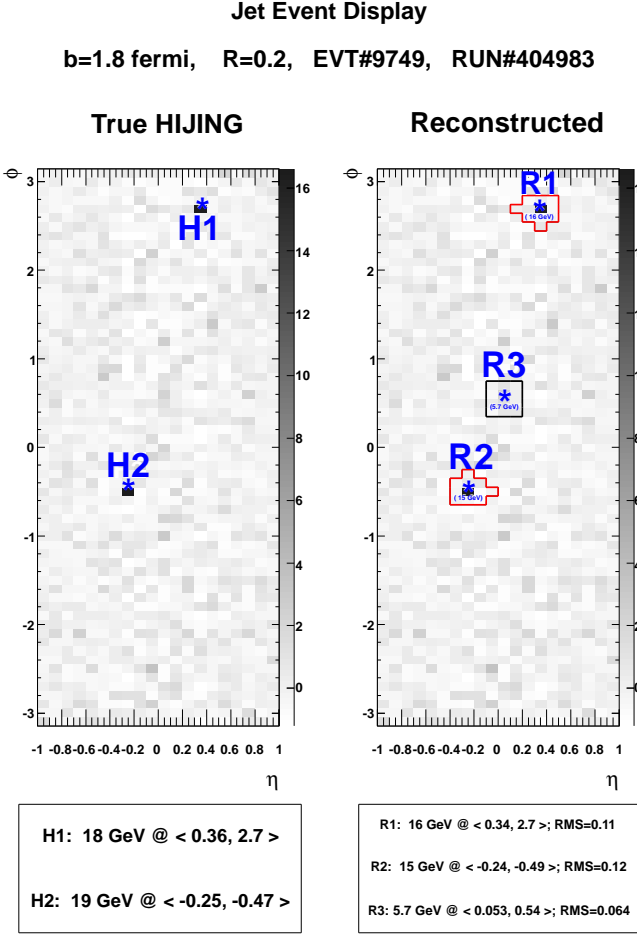


FIG. 2: Event display for a $E_T = 18$ GeV true dijet pair jet matched to a $E_T=15$ and 16 GeV reconstructed jets in a $b=1.8$ fm HIJING event. All jets shown in this event display are reconstructed with the anti- k_T algorithm with $R=0.2$. Both histograms show the background subtracted 0.1×0.1 $\eta - \phi$ tower energy. A minimum E_T cut of 5 GeV is placed on all jets shown in this display. The stars in the left panel show the true HIJING jets and box below shows jet E_T and η, ϕ location of the jet axis. The right panel shows the reconstructed jets. The jet labeled R1 is reconstructed at $E_T = 16$ GeV and matched to the H1 jet in the left panel and R2 is matched to H2. The other reconstructed jet in the event with $E_T > 5$ GeV is shown as R3. It is not associated with any true jets with $E_T > 5$ GeV.

tion of reconstructed jets are not matched at low E_T ; the fraction then falls quickly and goes below the matched reconstructed jets at around 18 GeV in the $R = 0.2$ case. The crossing point is at higher E_T for $R=0.3$ and 0.4 jets, around 25 and 30 GeV, respectively.

The low fake rate alone is not sufficient due to the arbitrariness of the 5 GeV separation between “fake” and “true” jet fragmentation associations. Shown in Figure 6 is the distribution of HIJING true energies for fully reconstructed jet energies (with different selections). The upper left panel for reconstructed jets with $R = 0.2$ and energies 15-20 GeV shows a peaked distribution around

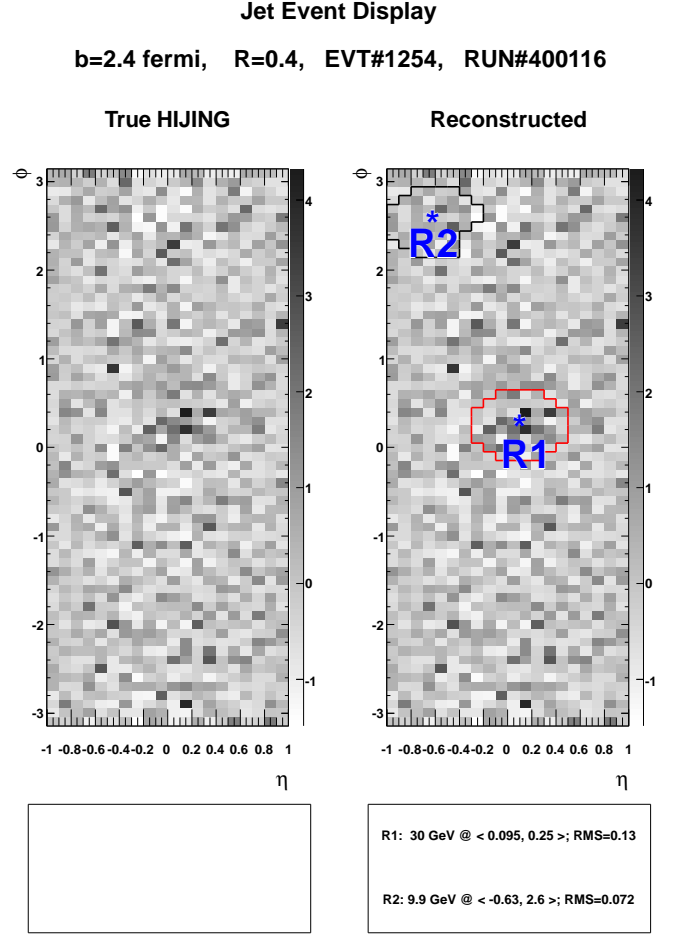


FIG. 3: Event display for a $E_T = 30$ GeV fake jet. All jets shown in this event display are reconstructed with the anti- k_T algorithm with $R=0.4$. Both histograms show the background subtracted 0.1×0.1 $\eta - \phi$ tower energy. A minimum E_T cut of 5 GeV is placed on all jets shown in this display. There are no true HIJING jets with $E_T > 5$ GeV in this event. The right panel shows the reconstructed jets. The jet labeled R1 is reconstructed at $E_T = 30$ GeV. The other reconstructed jet in the event with $E_T > 5$ GeV is shown as R2. The jet E_T and η, ϕ locations are shown in the bottom right box.

≈ 15 GeV. The tail to lower energies could in principle be accounted for in a response matrix (though with great care and systematic cross checks). However, as one moves to higher energies 25-30 GeV, there is essentially no tail contributions and a peak around 26 GeV and width of 5 GeV. This indicates a regime where a standard response matrix and unfolding procedure should be successful. Similar plots are shown for $R = 0.3$ and $R = 0.4$. There is a shift downward from the reconstructed jet energies to the corresponding true jet energies due to the rapid fall off of the jet cross section with energy and a tail to low HIJING jet energies that disappears with increasing reconstructed jet E_T and the corresponding decrease of fake jets.

In order to quantify the purity of the reconstructed jet

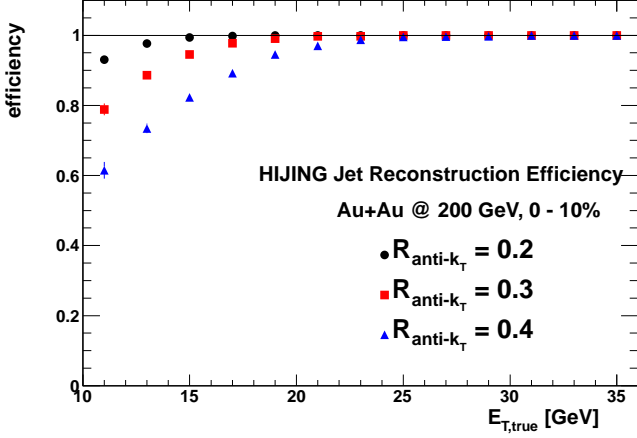


FIG. 4: Matching efficiency for true HIJING jets as a function of jet E_T for anti- k_T R parameters 0.2 (black), 0.3 (red) and 0.4 (blue). For a jet to be considered matched the reconstructed jet axis must be within $\Delta R < 0.25$ of the HIJING jet axis.

sample, we have fit the distributions with a background contribution which falls exponentially with increasing jet E_T and a Gaussian with a free mean and width. The results of those fits, along with the fractions of the total reconstructed jets (both matched and unmatched) which are included in the Gaussian are shown in Tables I-III.

$\langle E_{T, reco} \rangle$ (GeV)	$\langle E_{T, true} \rangle$ (GeV)	σ_{E_T}	$\frac{S}{S+B}$
17.19 ± 0.006017	14.57 ± 0.05368	3.765 ± 0.03063	0.2106
22.12 ± 0.0122	18.61 ± 0.0507	4.221 ± 0.0384	0.7446
27.19 ± 0.02707	24.09 ± 0.08153	3.788 ± 0.05263	0.8838
32.29 ± 0.05348	28.99 ± 0.1515	4.212 ± 0.1214	0.9248

TABLE I: Jet parameters from fits to the plots in Figure 6 for $R = 0.2$ anti- k_T jets with centrality from 0 - 10%. $\langle E_{T, reco} \rangle$ is the mean reconstructed jet E_T within the 5 GeV wide bins. $\langle E_{T, true} \rangle$ and $\sigma_{E_T, true}$ are the mean and width from the Gaussian component in the fit and $\frac{S}{S+B}$ is the fraction of the area of the fit that is included in the Gaussian component rather than the exponential.

$\langle E_{T, reco} \rangle$ (GeV)	$\langle E_{T, true} \rangle$ (GeV)	σ_{E_T}	$\frac{S}{S+B}$
22.1 ± 0.00748	14.9 ± 0.124	5.59 ± 0.0634	0.174
27.2 ± 0.0169	19.7 ± 0.179	5.83 ± 0.144	0.576
32.2 ± 0.0354	23.7 ± 0.261	6.33 ± 0.211	0.802
37.5 ± 0.072	29.6 ± 0.329	7.04 ± 0.306	0.908

TABLE II: Jet parameters from fits to the plots in Figure 7 for $R = 0.3$ anti- k_T jets with centrality from 0 - 10%. $\langle E_{T, reco} \rangle$ is the mean reconstructed jet E_T within the 5 GeV wide bins. $\langle E_{T, true} \rangle$ and $\sigma_{E_T, true}$ are the mean and width from the Gaussian component in the fit and $\frac{S}{S+B}$ is the fraction of the area of the fit that is included in the Gaussian component rather than the exponential.

In addition to the fake jet contribution to the reconstructed jet sample it is also important to quantify the

$\langle E_{T, reco} \rangle$ (GeV)	$\langle E_{T, true} \rangle$ (GeV)	σ_{E_T}	$\frac{S}{S+B}$
27.1 ± 0.01	15.5 ± 0.188	6.82 ± 0.119	0.128
32.2 ± 0.0222	20.3 ± 0.412	7.06 ± 0.258	0.417
37.3 ± 0.0469	25.6 ± 0.357	5.2 ± 0.427	0.379
42.4 ± 0.0987	30.4 ± 0.616	4.69 ± 0.726	0.444

TABLE III: Jet parameters from fits to the plots in Figure 8 for $R = 0.4$ anti- k_T jets with centrality from 0 - 10%. $\langle E_{T, reco} \rangle$ is the mean reconstructed jet E_T within the 5 GeV wide bins. $\langle E_{T, true} \rangle$ and $\sigma_{E_T, true}$ are the mean and width from the Gaussian component in the fit and $\frac{S}{S+B}$ is the fraction of the area of the fit that is included in the Gaussian component rather than the exponential.

jet energy resolution and scale for our algorithm. In order to do this we have embedded PYTHIA [25] (version 6.421) jets into our HIJING events. One PYTHIA event with a high p_T dijet was embedded into every HIJING event. The PYTHIA and reconstructed jets are required to obey the same matching cut of $\Delta R < 0.25$ as the fake jet study discussed above. The jet energy resolution and jet energy scale are shown in Figure 9 the anti- k_T R parameters 0.2 and 0.4 for central HIJING events and PYTHIA events (not embedded into HIJING) put into towers in the same manner as the HIJING events. The jet energy resolution improves with increasing jet energy and decreasing jet R as expected. The energy scale, $\frac{\langle E_{T, reco} - E_{T, true} \rangle}{E_{T, true}}$ is within $\approx 5\%$ of zero for the anti- k_T R parameters considered here. The energy offset for the PYTHIA jets is due to the imposed tower segmentation. For the purposes of this study we did not pursue further refinements. A similar resolution evaluation has been done by the CMS collaboration [4].

V. CONCLUSIONS

We have performed a HIJING study of jet reconstruction using an iterative background subtraction method and full calorimetric information. We have shown that in this case we are able to reconstruct the input HIJING jets with a large signal to background with $E_T > 20$ GeV for $R = 0.2$ jets, 30 GeV for $R = 0.3$ jets and 40 GeV for $R = 0.4$ jets. The results presented here are obtained without any additional rejection of fake jets, though it is possible the reconstructed jet purities shown here could be further increased with fake jet rejection of some kind.

This study was designed to evaluate the feasibility of purely calorimetric jet measurements at RHIC. The results here are obtained using an ideal model of the detector and suggest promise for such measurements. This study is of course limited in scope. We have not taken into effect any detector effects aside from geometrical acceptance and granularity. More detailed studies need to be done to demonstrate the suitability of any particular detector design for jet measurements.

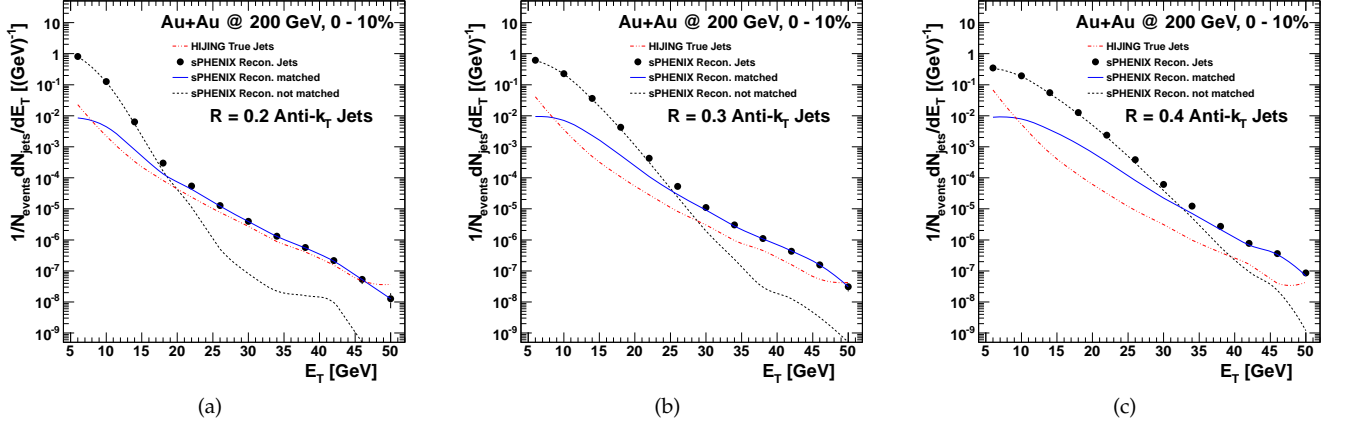


FIG. 5: E_T spectra for true HIJING jets (red line) and reconstructed jets (black points). The reconstructed jets are further divided into those which are matched to a true HIJING jet (blue line) and those which are not matched to a true HIJING jet (“fake jets”, black line). To be considered matched the axis of the true HIJING jet and the reconstructed jet must be within $\Delta R < 0.25$ and the HIJING jet must have $E_T > 5$ GeV. Shown are results for 0-10% central HIJING events using anti- k_T jets with $R=0.2$ (a), $R=0.3$ (b) and $R=0.4$ (c).

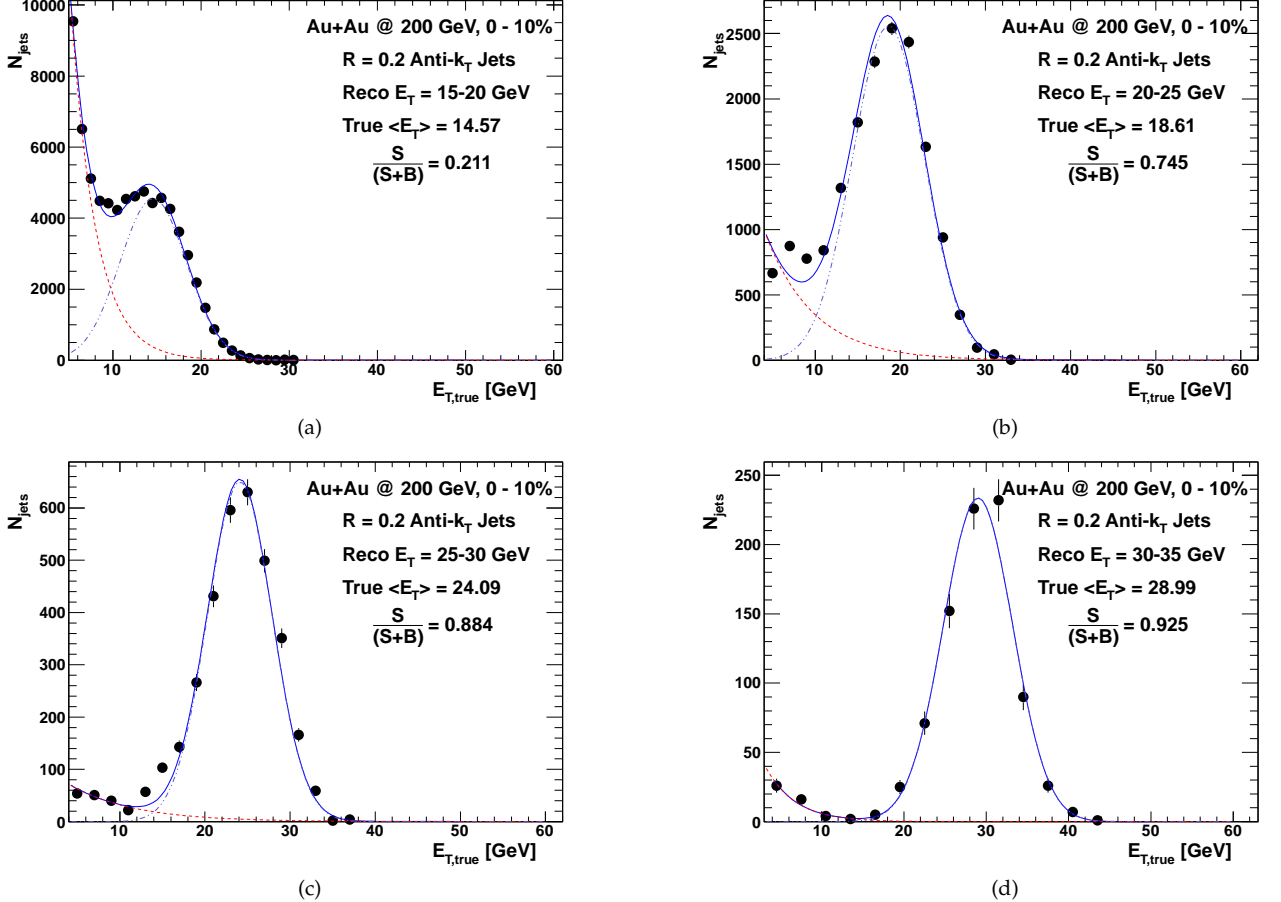


FIG. 6: True E_T for reconstructed jets anti- k_T $R = 0.2$ for the reconstructed jet E_T 15-20 GeV (a), 20-25 GeV (b), 25-30 GeV (c) and 35-40 GeV (d). The lines show the results of fits containing a background component which is exponentially falling (dashed line) and a signal Gaussian component (dot-dashed line). The total fit is shown as a solid line. The plots show the $\frac{S}{S+B}$ where the signal (S) is determined from the area under the Gaussian within $\pm 2\sigma$ of the mean and the total background (B) includes both those jets reconstructed with a $> 2\sigma$ energy mismatched and those which were not matched at all to a HIJING jet. Fit parameters are shown in Table I.

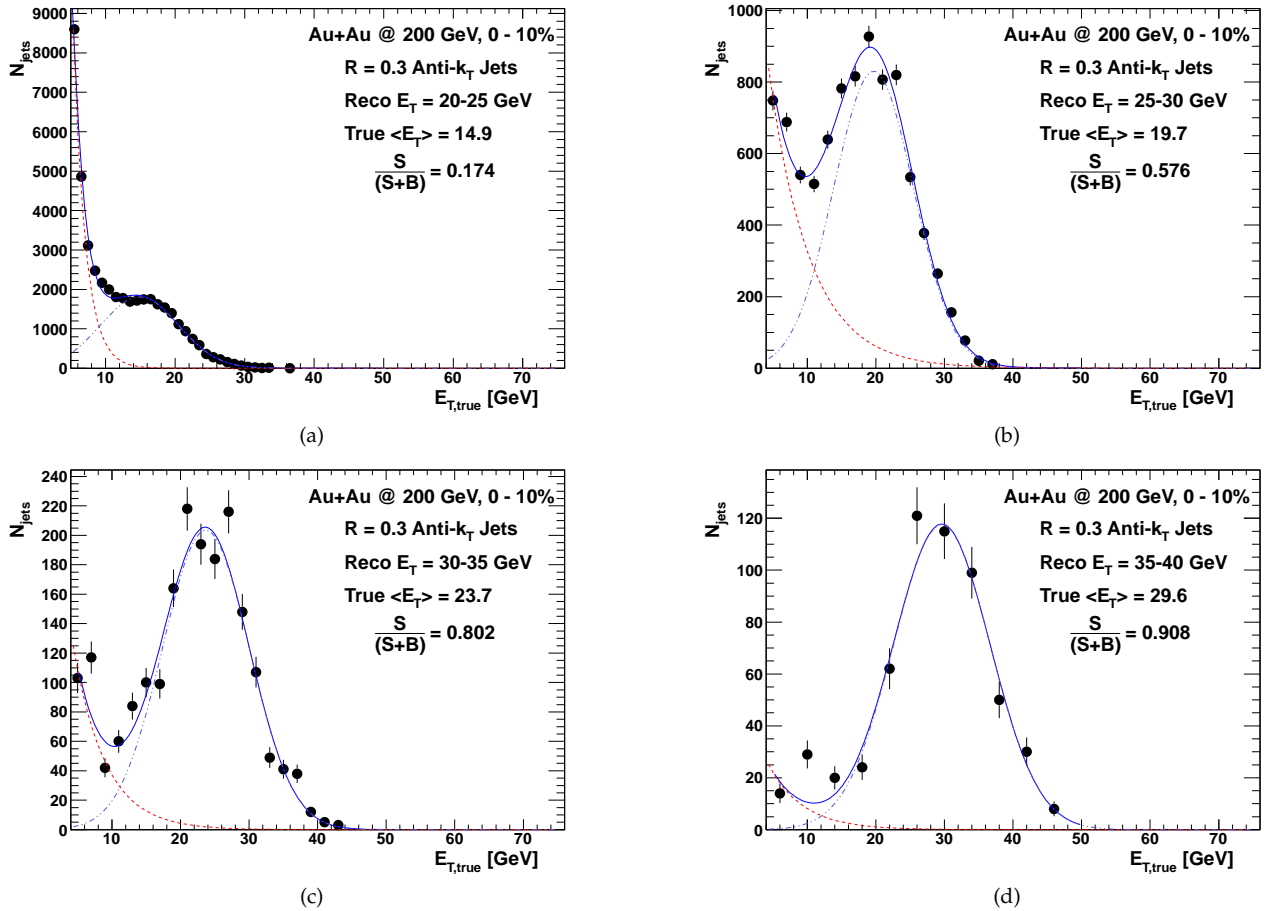


FIG. 7: True E_T for reconstructed jets anti- k_T $R = 0.3$ for the reconstructed jet E_T 20-25 GeV (a), 25-30 GeV (b), 30-35 GeV (c), 35-40 GeV (d). The lines show the results of fits containing a background component which is exponentially falling (dashed line) and a signal Gaussian component (dot-dashed line). The total fit is shown as a solid line. The plots show the $\frac{S}{S+B}$ where the signal (S) is determined from the area under the Gaussian within $\pm 2\sigma$ of the mean and the total background (B) includes both those jets reconstructed with a $> 2\sigma$ energy mismatched and those which were not matched at all to a HIJING jet. Fit parameters are shown in Table II.

VI. ACKNOWLEDGMENTS

Funding has been provided from the Department of Energy under contract number DE-AC02-98CH10886

(A.M.S, A.F, D.P.M, C.H.P, and P.S) and grant numbers DE-FG02-96ER40988 (J.A.H, B.S.,M.vS) and DE-FG02-03ER41244 (M.P.M, J.L.N, M.S).

-
- [1] M. Gyulassy and X. Wang, Comput. Phys. Commun. **83**, 307 (1994), nucl-th/9502021.
 - [2] ATLAS (ATLAS Collaboration) (2011), URL cdsweb.cern.ch/record/1353220/files/ATLAS-CONF-2011-073.
 - [3] G. Aad et al. (Atlas Collaboration), Phys.Rev.Lett. **105**, 252303 (2010), 1011.6182.
 - [4] S. Chatrchyan et al. (CMS Collaboration), Phys.Rev. **C84**, 024906 (2011), 1102.1957.
 - [5] K. Adcox et al. (PHENIX), Phys. Rev. Lett. **88**, 022301 (2002), nucl-ex/0109003.
 - [6] A. Adare et al. (PHENIX), Phys. Rev. Lett. **101**, 232301 (2008), 0801.4020.
 - [7] J. Adams et al. (STAR Collaboration), Phys.Rev.Lett. **91**, 172302 (2003), nucl-ex/0305015.
 - [8] J. Adams et al. (STAR Collaboration), Phys.Rev.Lett. **97**, 162301 (2006), nucl-ex/0604018.
 - [9] A. Adare et al. (PHENIX Collaboration), Phys.Rev. **C78**, 014901 (2008), 0801.4545.
 - [10] B. Abelev et al. (STAR Collaboration), Phys.Rev. **C80**, 064912 (2009), 0909.0191.
 - [11] A. Adare et al. (PHENIX), Phys. Rev. Lett. **104**, 252301 (2010), 1002.1077.
 - [12] X.-N. Wang, Z. Huang, and I. Sarcevic, Phys.Rev.Lett. **77**, 231 (1996), hep-ph/9605213.
 - [13] P. Steinberg and A. Collaboration (2011), 1110.3352.
 - [14] A. Majumder and M. Van Leeuwen (2010), 1002.2206.

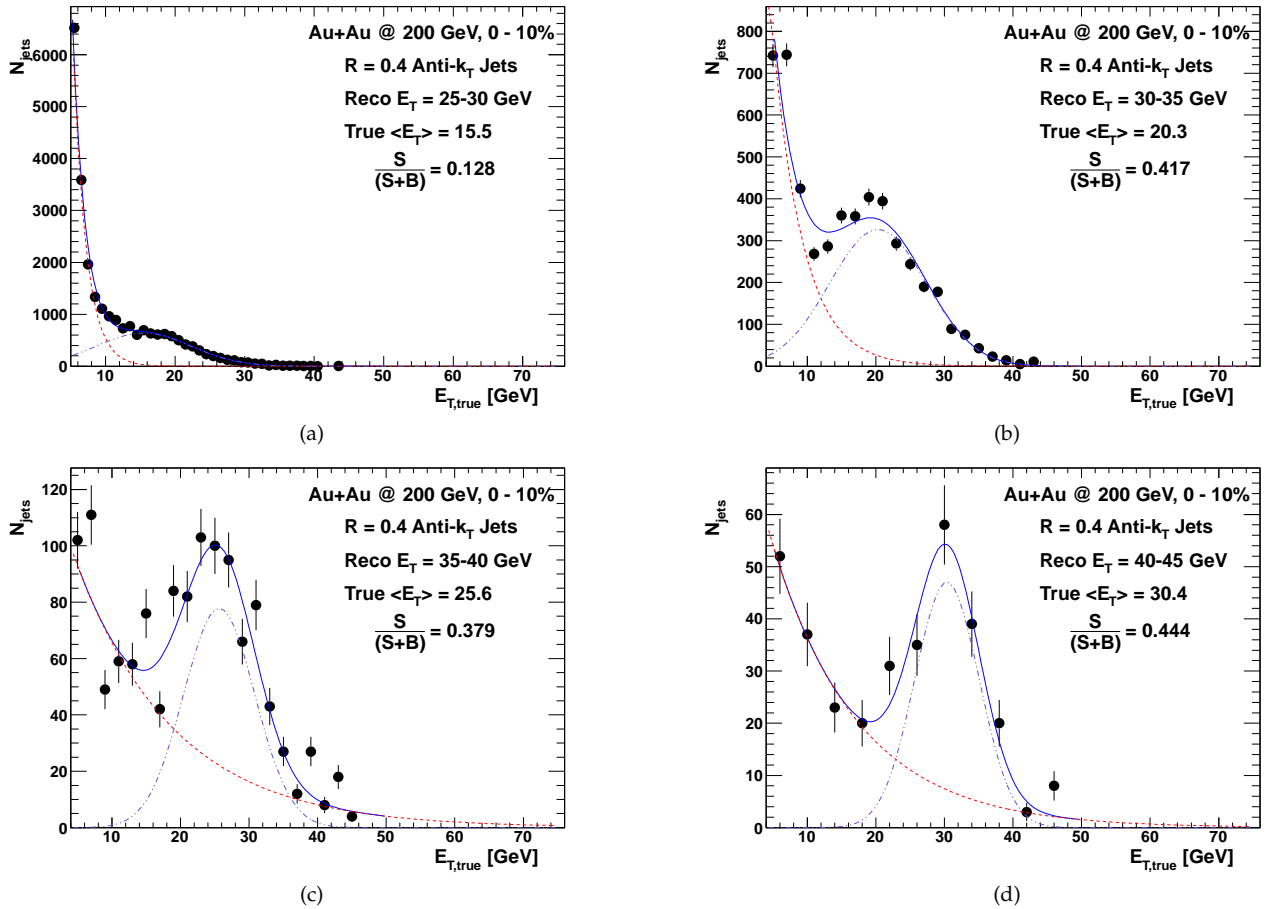


FIG. 8: True E_T for reconstructed jets anti- k_T $R = 0.4$ for the reconstructed jet E_T 25-30 GeV (a), 30-35 GeV (b), 35-40 GeV (c), 40-45 GeV (d). The lines show the results of fits containing a background component which is exponentially falling (dashed line) and a signal Gaussian component (dot-dashed line). The total fit is shown as a solid line. The plots show the $\frac{S}{S+B}$ where the signal (S) is determined from the area under the Gaussian within $\pm 2\sigma$ of the mean and the total background (B) includes both those jets reconstructed with a $> 2\sigma$ energy mismatched and those which were not matched at all to a HIJING jet. Fit parameters are shown in Table III.

- [15] K. Aamodt et al. (ALICE Collaboration), Phys.Rev.Lett. **106**, 032301 (2011), 1012.1657.
- [16] M. Cacciari, G. P. Salam, and G. Soyez, Eur.Phys.J. **C71**, 1692 (2011), 1101.2878.
- [17] B. Abelev et al. (ALICE Collaboration) (2012), 1201.2423.
- [18] P. Jacobs (STAR Collaboration) (2010), 1012.2406.
- [19] W. Vogelsang, private communication.
- [20] PHENIX (2010), URL http://www.phenix.bnl.gov/phenix/WWW/docs/phenix_decadal10_full_refs.pdf.
- [21] M. Cacciari, G. Salam, and G. Soyez, JHEP **0804**, 063 (2008), 0802.1189.
- [22] M. Cacciari and G. P. Salam, Phys.Lett. **B641**, 57 (2006), hep-ph/0512210.
- [23] M. Masera, G. Ortona, M. Poghosyan, and F. Prino, Phys. Rev. **C79**, 064909 (2009).
- [24] A. Adare et al. (PHENIX Collaboration), Phys.Rev.Lett. **107**, 252301 (2011), 1105.3928.
- [25] T. Sjostrand et al., Comput. Phys. Commun. **135**, 238 (2001), hep-ph/0010017.

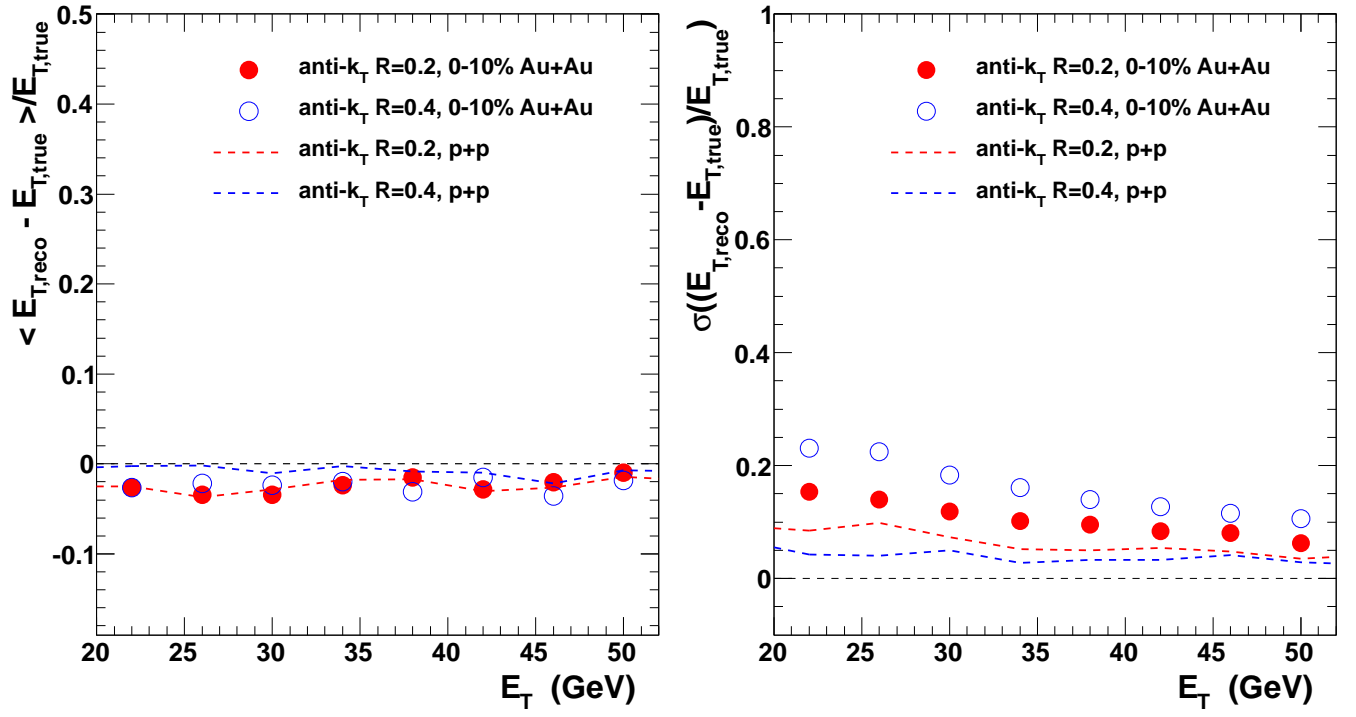


FIG. 9: Jet energy resolution as a function of the true jet energy for jets reconstructed in 0-10% central HIJING events. Shown in the plot are anti- k_T $R = 0.2$ (black), $R = 0.3$ (red) and $R = 0.4$ (blue).